J. Phys. Chem. Solids Vol. 50, No. 2, pp. 163–170, 1989
Printed in Great Britain.

0022-3697/89 $3.00 + 0.00

FTIR ELECTRONIC SPECTRA OF $Fe_2P_2S_6$ AND $Co_2P_2S_6$: TRIGONAL FIELD SPLITTING AND LITHIUM INTERCALATION EFFECTS

N. NAGASUNDARAM and A. H. FRANCIS
Department of Chemistry, University of Michigan, Ann Arbor, MI 48109, U.S.A.

(*Received* 20 *June* 1988; *accepted* 20 *September* 1988)

Abstract—The FTIR electronic absorption spectra of single crystals of $Fe_2P_2S_6$, $Co_2P_2S_6$ and their lithium intercalation compounds have been obtained. The spectrum of $Fe_2P_2S_6$ exhibits a broad, weak absorption feature at 1885 cm^{-1} and a second, stronger band at 8870 cm^{-1}. These are assigned to transitions between the ^5E_g (ground state) and the $^5A_{1g}$ and ^5E_g trigonal crystal-field components of the Fe^{2+} free-ion ^5D ground term. The broad absorption bands in the spectrum of $Co_2P_2S_6$ are assigned to the transitions between the $^4A_{2g}$ (ground state) and the ^4E_g (1224 cm^{-1}) and $^4A_{1g}$ (7124 cm^{-1}) trigonal crystal-field components of the Co^{2+} free-ion ^4F ground term. A point-charge crystal-field model was used to relate the crystal-field splitting parameters (Dq and Cp) to the trigonal lattice distortion.

Lithium intercalation completely suppresses the trigonal field transition in $Co_2P_2S_6$ and causes a dramatic shift of the absorption edge to lower frequencies. However, lithium intercalation has little effect upon the spectrum of $Fe_2P_2S_6$.

Keywords: $Fe_2P_2S_6$, $Co_2P_2S_6$, FTIR, electronic absorption, trigonal splitting, lithium intercalation, crystal-field model, trigonal angle.

INTRODUCTION

The $M_2P_2S_6$ (M = a first row transition metal) materials form a large family of layered compounds with isomorphous crystal structures in which the coordination geometry of the M^{2+} ions is that of a trigonally distorted octahedron [1]. The weak interlayer van der Waals forces permit the lattice to be intercalated by a wide range of chemical species. The intercalation of these lattices with alkali metals, in particular, has been investigated for more than a decade. The electronic band structure of both the host lattices and the intercalated lattices have been examined experimentally and theoretically in order to develop an understanding of the physical and chemical behavior of these interesting materials.

The electronic absorption spectra in the region of the electronic band gap can provide detailed information about the host lattice band structure and the changes produced by intercalation. For lattices containing transition metal ions with partially filled d-orbitals, the long-wavelength electronic absorption spectrum arises from the $d \leftarrow d$ transitions of the transition metal ion [2–7]. If the d-orbitals are weakly overlapping, then these excitations may be viewed as localized crystal field transitions; if the interaction between d-orbitals is substantial, then the transitions should be viewed as between delocalized d-bands. In either case, the d-orbitals are split by the octahedral crystal field into a high-energy e_g set (d_{xz}, d_{yz}) and a low-energy t_{2g} set ($d_{x^2-y^2}$, d_{xy}, d_{z^2}). Because the coordination of the transition metal ion in the $M_2P_2S_6$ lattices is trigonally distorted (D_{3d}), the t_{2g} orbital set is further split into an a_{1g} (d_{z^2}) and an e_g orbital pair ($d_{x^2-y^2}$, d_{xy}). The z-axis is taken as the trigonal axis of the MS_6 octahedron and coincides with the crystallographic c^*-axis (see Fig. 1).

The trigonal field splitting may affect the physical properties of the $M_2P_2S_6$ materials since these will depend upon the energy of thermally accessible electronic states and the density of states at the Fermi energy. Moreover, the trigonal field splitting should be sensitive to intercalation induced changes in both the metal coordination geometry and the strength of the metal–chalcogen bond. Relatively little is known about the structural modifications of the host lattice induced by the intercalate, and the behavior of the trigonal field splitting upon lattice intercalation may be helpful in the interpretation of electronic and structural changes caused by the intercalate.

We have previously reported the FTIR spectra of several $M_2P_2X_6$ (M = Cd, Mn, Fe, Co) compounds and identified a broad, weak absorption band in the spectra of $Fe_2P_2S_6$ and $Co_2P_2S_6$ with the electronic transition between the trigonal components of the free-ion, ground state term [8]. In the present work, we have extended our earlier measurements to a wider spectral range to observe additional crystal field transitions and examined the corresponding spectra of lithium intercalated lattices.

EXPERIMENTAL

Single crystals of $Fe_2P_2S_6$ and $Co_2P_2S_6$ were prepared by direct synthesis from the elements in evacuated quartz tubes. The details of the procedure have been described previously [9, 10]. Elemental analyses

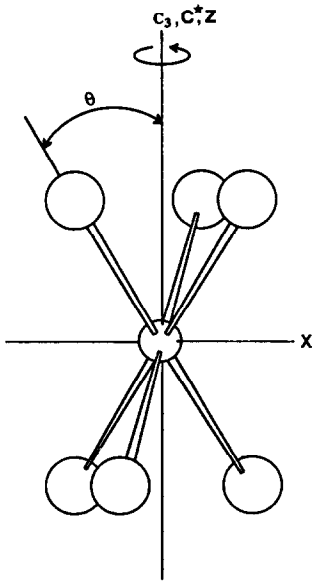

Fig. 1. Axis notation and orientation of the trigonal axis with respect to the crystallographic stacking axis c^*. θ is the trigonal distortion angle.

and the basal plane spacings determined by single crystal X-ray diffraction were consistent with previously published data for all materials studied. Lithium intercalation was carried out in a nitrogen atmosphere in dried Schlenkware using *n*-butyllithium in hexane solution. The detailed procedure has been described previously [11]. The time of intercalation was varied from 1 to 10 h in order to obtain a variation in the amount of intercalated lithium.

FTIR spectra were recorded on a Nicolet 60SX spectrometer equipped with a microbeam attachment and optional beam-splitters to extend the high-energy operating range to 25,000 cm^{-1}. Single crystals about 0.1 mm thick were mounted across a 1 mm circular aperture. All spectra were recorded at room temperature with the incident radiation perpendicular to the basal cleavage of the sample. Typically, 300 scans were collected for each spectrum.

RESULTS

The FTIR spectrum of $Fe_2P_2S_6$ is illustrated in Fig. 2. Most of the sharp line features correspond to vibrational transitions associated with P–S and Fe–S deformations [12, 13]. The spectrum exhibits two weak, broad absorption bands whose peak intensities are very much less than that of fundamental vibrational absorption bands, but comparable to higher overtone intensities. The first of these features is observed at 1885 cm^{-1} and has a full width at half-maximum (FWHM) of 1350 cm^{-1}. The second band is observed at 8870 cm^{-1} with a FWHM of 3240 cm^{-1}.

The FTIR spectrum of $Co_2P_2S_6$ is shown in Fig. 3 and, like the spectrum of $Fe_2P_2S_6$, exhibits two broad absorption features (1224 cm^{-1}, FWHM = 830 cm^{-1} and 7124 cm^{-1}, FWHM = 1995 cm^{-1}). The band centered at 7124 cm^{-1} appears to consist of two overlapping bands.

The peak molar extinction coefficients were determined for each electronic transition observed. The thickness of the sample crystals was measured optically with a metallurgical microscope. The sample crystal density for $Co_2P_2S_6$ was obtained by calcu-

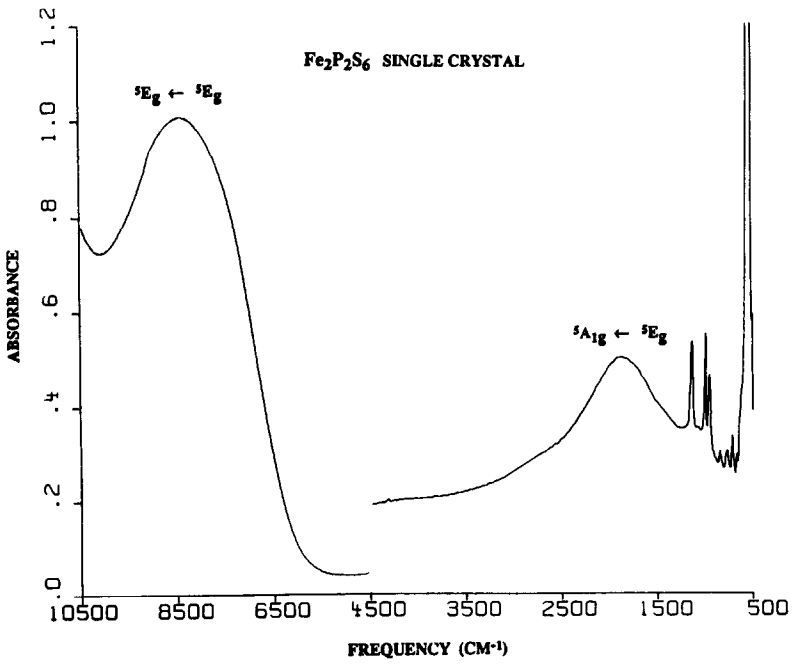

Fig. 2. Single crystal absorption spectrum of $Fe_2P_2S_6$.

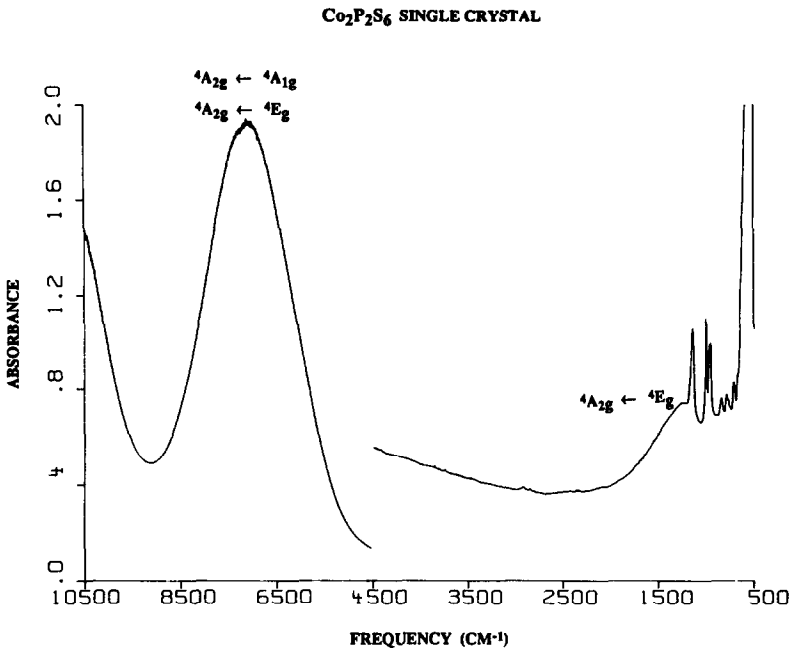

Fig. 3. Single crystal absorption spectrum of $Co_2P_2S_6$.

lation from the unit cell dimensions [14], while for $Fe_2P_2S_6$ the average value given in Ref. 10 was used. The peak molar absorption coefficient values obtained for both sample materials are reported in Table 1.

The spectra of lithium intercalation compounds of $Fe_2P_2S_6$ and $Co_2P_2S_6$ are compared in Fig. 4. As noted in previous studies, when single crystals of $Fe_2P_2S_6$ and $Co_2P_2S_6$ are intercalated with lithium, the vibrational spectrum in the spectral range 400–1500 cm^{-1} is only slightly altered [15]. In the spectral range $>1500\ cm^{-1}$, very little change occurs in the spectrum of $Li_xFe_2P_2S_6$ relative to that of the host lattice. The spectrum of $Li_xCo_2P_2S_6$, however, is altered dramatically at frequencies greater than 1200 cm^{-1}. The trigonal field transition disappears and a strong absorption edge appears at about 3000 cm^{-1}.

DISCUSSION

The long-wavelength transitions of the $M_2P_2X_6$ materials with partially filled *d*-orbitals are expected to involve contributions from *d*-orbital transitions. As an aid to interpretation of the long-wavelength spectrum, it would be desirable to have available a calculation of the optical joint density of states for the $M_2P_2X_6$ lattices. Although these are not available, extended Huckel tight-binding analyses of the electronic structure of the $M_2P_2S_6$ phases have recently

Table 1.

Parameter	$Fe_2P_2S_6$	$Co_2P_2S_6$	Units
Ground state	^5E_g	$^4A_{2g}$	
1st excited	$^5A_{1g}$	^4E_g	
Energy	1885	1224	cm^{-1}
Linewidth (FWHM)	1350	830	cm^{-1}
Peak extinction	2	6	$l(mol\text{-}cm^{-1})^{-1}$
2nd excited	^5E_g	$^4A_{1g}$	
Energy	8870	7124	cm^{-1}
Linewidth (FWHM)	3240	1995	cm^{-1}
Peak extinction	7	33	$l(mol\text{-}cm^{-1})^{-1}$
Trigonal angle	51.27	51.52	deg
Dq	770	837	cm^{-1}
Cp	2797	5350	cm^{-1}
$\frac{\delta E_{A1g}}{\delta\theta}$	−626	−36	$cm^{-1}\,deg^{-1}$
$\frac{\delta E_{Eg}}{\delta\theta}$	−228	−492	$cm^{-1}\,deg^{-1}$

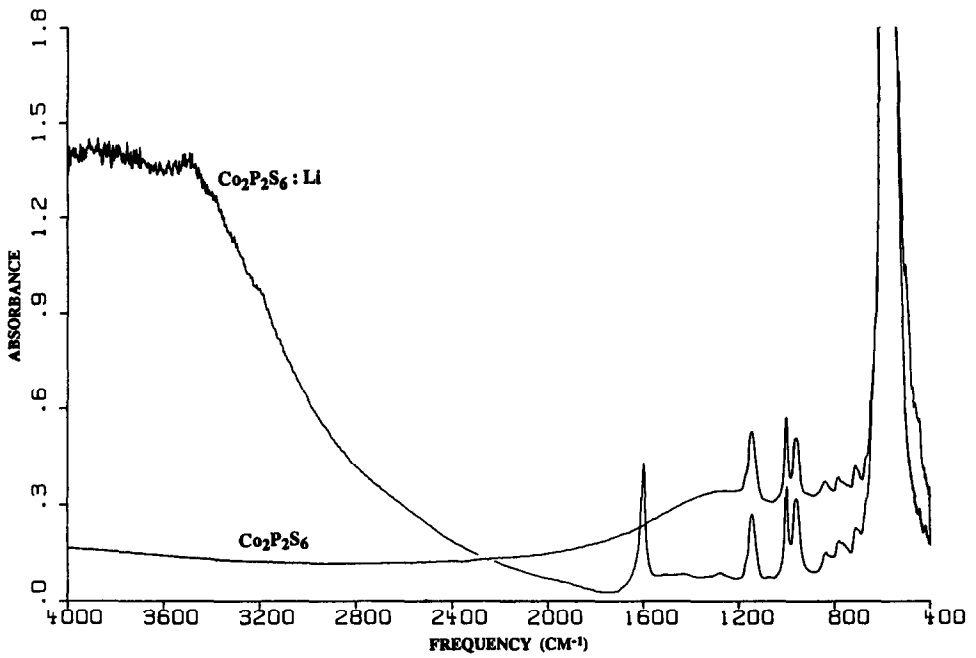

Fig. 4. Comparison of the absorption spectra of $Co_2P_2S_6$ and $Li_xCo_2P_2S_6$.

been reported by Whangbo *et al.* for M = Fe [16] and by Mercier *et al.* for M = Mn, Fe, Co, Ni [17]. These calculations indicate considerable mixing of the *d*-orbital t_{2g} set with P–P orbitals due to the presence of the trigonal distortion of the metal coordination. Since these calculations also indicate relatively little dispersion of the t_{2g} orbitals, favoring localization of the *d*-orbitals, we have adopted simple crystal field arguments (for isolated transition metal ions in trigonal coordination) for the present discussion of the mid-IR electronic spectra of $Fe_2P_2S_6$, $Co_2P_2S_6$ and their lithium intercalation compounds [8].

Crystal-field splitting

A trigonal distortion in the MS_6 octahedra in $M_2P_2S_6$ crystals results, as mentioned earlier, in a splitting of the *d*-orbitals into d_{z^2} (t_{2g}^0), $d_{x^2-y^2}$ and d_{xy} ($t_{2g}^{\pm}$), and d_{xz} and d_{yz} (e_g). Although the e_g set is always higher in energy than the t_{2g} set, the ordering within the t_{2g} set depends on the trigonal angle, defined in Fig. 1, and the relative magnitudes of *Dq* and *Cp*, the cubic and the trigonal crystal field splittings, respectively. Consequently, there are two possible orderings of the *d*-orbitals (see Fig. 5).

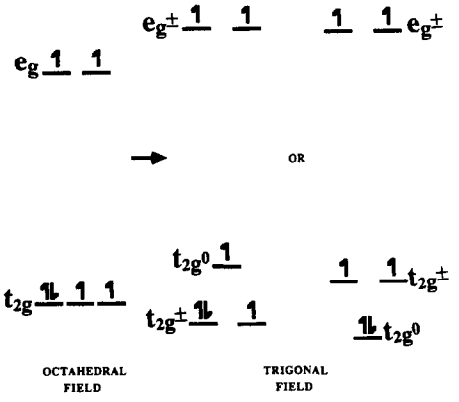

Fig. 5. Splitting of the 3*d* transition metal orbitals in a trigonal crystal field.

The ^5D free-ion electronic ground term of high spin Fe^{2+} in $Fe_2P_2S_6$ corresponds to the electronic configuration, $t_{2g}^4e_g^2$ in the cubic field. In the trigonal field, the orbital configuration becomes either $(t_{2g}^{\pm})^3(t_{2g}^0)^1(e_g)^2$, corresponding to a ^5E_g state, or $(t_{2g}^0)^2(t_{2g}^{\pm})^2(e_g)^2$, corresponding to a $^5A_{1g}$ state, as shown in Fig. 5. In either case, a spin-allowed trigonal transition within the t_{2g} set is possible: $^5A_{1g}\{(t_{2g}^{\pm})^2(t_{2g}^0)^2(e_g)^2\} \leftarrow {}^5E_g$ or $^5E_g\{(t_{2g}^0)^1(t_{2g}^{\pm})^3(e_g)^2\} \leftarrow {}^5A_{1g}$. It is this transition that gives rise to the 1885 cm^{-1} band observed in the mid-IR electronic absorption spectrum of $Fe_2P_2S_6$. The next higher-energy, spin-allowed transition leads to the configuration $(t_{2g}^{\pm})^2(t_{2g}^0)^1(e_g)^3$ or $(t_{2g}^0)^1(t_{2g}^{\pm})^2(e_g)^3$. We assign the 8870 cm^{-1} band observed in the near-IR spectrum of $Fe_2P_2S_6$ to this $^5E_g \leftarrow {}^5E_g$ or $^5E_g \leftarrow {}^5A_{1g}$ transition.

In a similar fashion the octahedrally split $t_{2g}^5e_g^2$ configuration corresponding to the free-ion ^4F electronic ground term of Co^{2+} is further split by the trigonal field in $Co_2P_2S_6$ into a $^4A_{2g}$ state, or into $(t_{2g}^0)^2(t_{2g}^{\pm})^3(e_g)^2$, a ^4E_g state, depending again on the splitting of the t_{2g} set. Either of these configurations gives rise to a spin-allowed transition which is $^4A_{2g} \leftarrow {}^4E_g$ or $^4E_g \leftarrow {}^4A_{2g}$. We have assigned the 1224 cm^{-1} band to this transition. We assign the

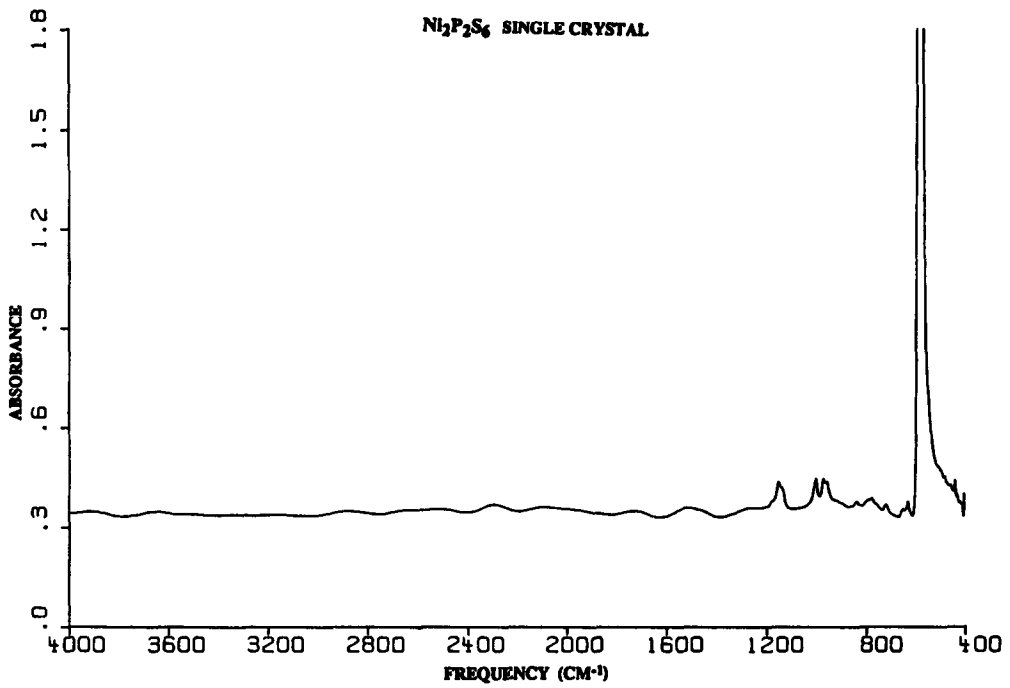

Fig. 6. Single crystal absorption spectrum of $Ni_2P_2S_6$.

7124 cm^{-1} band to the transition involving the promotion of an electron from the t_{2g} orbital set or t_{2g}^0 orbital to the e_g orbital set, that is, $^4A_{1g} \leftarrow {}^4A_{2g}$ or $^4A_{1g} \leftarrow {}^4E_g$.

The band positions, linewidths and intensities observed in the IR electronic absorption spectra of $Fe_2P_2S_6$ and $Co_2P_2S_6$ (see Table 1) are consistent with the values expected for (electronic) crystal-field transitions between the trigonal field components of the ground free-ion term. For the d^8 configuration of Ni^{2+} in $Ni_2P_2S_6$, the t_{2g} orbital set is completely filled and a single electron excitation within the t_{2g} set is not possible. No electronic absorption band was observed in the FTIR spectrum of this material (Fig. 6).

Point-charge crystal-field model

The orbital degeneracy of the electronic ground state cannot be determined from analysis of the spectrum alone. In order to conveniently examine the behavior of the ground state as a function of the trigonal field, we have adopted a point-charge model of the metal coordination. The model permits estimation of Dq and Cp by fitting the predicted crystal-field levels to the experimentally observed band positions, using the empirically found trigonal angle in $Fe_2P_2S_6$ and $Co_2P_2S_6$.

The point-charge model [18–20] provides a useful representation of the trigonally distorted crystal-field potential that permits parameterization in terms of the three separable parameters: the trigonal angle (θ), the cubic field splitting parameter (Dq), and the trigonal field splitting parameter (Cp). The above parameterization of the crystal field allows computation of the energy levels as a function of the trigonal distortion angle and the magnitude of the Dq and Cp parameters. The magnitude of the Dq parameter is proportional to the fourth-order radial one-electron integral $\langle r^4 \rangle$ and is given by,

$$Dq = \frac{\frac{1}{6} Ze^2 \langle r^4 \rangle}{a^5}. \quad (1)$$

Cp parameterizes second-order radial integrals of the form $\langle r^2 \rangle$ and is given by,

$$Cp = \frac{\frac{2}{7} Ze^2 \langle r^2 \rangle}{a^3}. \quad (2)$$

The crystal-field potential for D_{3d} trigonal symmetry may be written in terms of these parameters as:

$$V_{D_{3d}} = 21\sqrt{\pi/5}\, Cp[3\cos^2\theta - 1]Y_2^0 + 3\sqrt{\pi}\, Dq[35\cos^4\theta - 30\cos^2\theta + 3]Y_4^0 + 3\sqrt{35\pi}\, Dq[\sin^3\theta - \cos\theta][Y_4^3 - Y_4^{-3}], \quad (3)$$

where the Y_l^m are spherical harmonics of order l. Diagonalization of the matrix of the crystal-field Hamiltonian using the potential of eqn (3) leads directly to the energy levels of the ground state free-ion term split by the cubic and trigonal crystal-field components. A further smaller splitting is induced by the spin–orbit coupling.

For Fe^{2+}, the crystal-field Hamiltonian was diagonalized using the 25 basis functions $|L, M_l, S, M_s\rangle$ for the ^5D state ($L = 2, S = 2$) constructed from

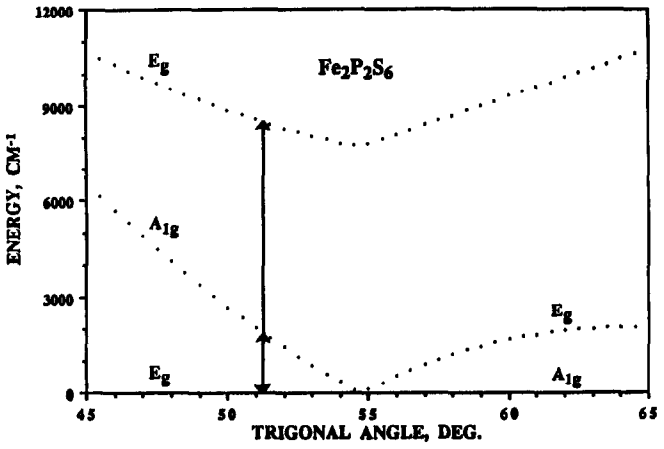

Fig. 7. Variation of the crystal-field splitting as a function of the trigonal angle.

one-electron d-orbital functions. For Co^{2+} it is necessary to consider spin–orbit coupling of the ^4F ground state with the nearby ^4P free-ion excited state. The crystal-field Hamiltonian was diagonalized using the 28 functions of the decoupled basis $|L, M_l, S, M_s\rangle$ for the ^4F-state ($L = 3, S = 3/2$), and 12 basis functions for the ^4P-state ($L = 1, S = 3/2$), constructed from one-electron d-orbital functions. The values of other parameters used in the calculation for $Co_2P_2S_6$ were B(Racah) = 500 cm^{-1} and ξ (molecular spin–orbit coupling parameter) = -100 cm^{-1}.

The value of the trigonal angle θ in crystalline $Fe_2P_2S_6$ was computed from recent refinements of the crystal structure [14]. The value obtained is $\theta_{cryst} = 51.3°$, corresponding to an elongation along the trigonal axis of the sulfur octahedron.

Dq and Cp were computed iteratively by repeated diagonalization of the matrix of the Hamiltonian with $\theta = \theta_{cryst.}$ until agreement with the observed band positions was obtained. The values of Dq and Cp obtained from this procedure were then used to generate the plot of the crystal-field levels of $Fe_2P_2S_6$ as a function of the trigonal distortion (Fig. 7). For values less than 54.7°, corresponding to octahedral coordination the ground state is the ^5E_g component of the $^5T_{1g}$; whereas for values greater than this, the $^5A_{1g}$ component lies lowest.

This result is in agreement with the Mössbauer measurements which suggest that the iron in $Fe_2P_2S_6$ is high-spin Fe^{2+} and that the ground state is ^5E_g [21]. Additionally, the very weak temperature dependence of the Mössbauer quadrupole splitting implies that the trigonal distortion about Fe^{2+} is moderately large. The ratio of $Cp/Dq = 3.63$ found in $Fe_2P_2S_6$ is typical of many ferrous salts which exhibit ratios near four.

For $Co_2P_2S_6$, $\theta_{cryst.} = 51.5°$ [14]. Dq and Cp were determined iteratively by repeated diagonalization of the crystal-field Hamiltonian with the potential of eqn (3) until agreement with the spectroscopic trigonal splittings was obtained. The final values of Dq and Cp (see Table 1) were then used to plot the variation of the trigonal field splitting vs θ illustrated in Fig. 8. The calculation predicts that for $\theta_{cryst.}$, the ground

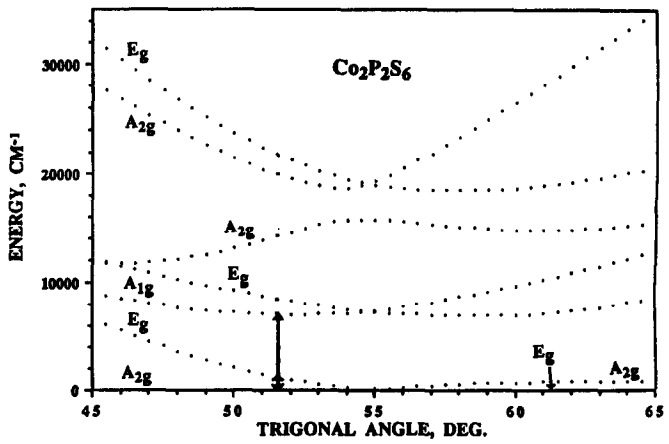

Fig. 8. Variation of the crystal-field splitting as a function of the trigonal angle.

electronic state is the $^4A_{2g}$ state. The Cp/Dq ratio is 6.39 and is typical of many cobalt salts [20].

It was found that trigonal splitting is sensitive to changes in the trigonal angle, but relatively insensitive to changes in Dq and Cp. The sensitivity is given by the parameter values in the last two rows of Table 1. This behavior has been noted previously [20] and is reflected in the dramatic sensitivity of the mean magnetic moment of trigonally distorted octahedral Fe^{2+} and Co^{2+} complexes to slight changes in coordination geometry. The most marked effects are observed when Cp is large and $\theta < \theta_{oct.} = 54.7°$.

Lithium intercalation effects on the FTIR electronic spectrum

Lithium can be inserted relatively easily into the $M_2P_2S_6$ lattices with partially filled d-bands (M = Ni, Fe, Co), but only with difficulty into lattices with filled d-bands (M = Cd, Zn). It is usually assumed that intercalation of a layer compound does not modify the intralayer structure of the host, but only alters the interlayer separation. This is not necessarily the case as illustrated by the effect of Na intercalation into TiS_2. The ^{23}Na Knight shift measurements [22] indicate that intercalation flattens each TiS_2 layer and shortens the interlayer separation. Flattening of a layer may be assumed to involve an increase in the trigonal distortion angle θ, rather than a shortening of the strong, covalent M–S bond. Tight-binding band structure calculations, using θ to parameterize the intralayer deformation, indicate that a small change in the trigonal angle significantly modifies the lowest lying d-band [23]. For $\theta < 54.9°$, the lowest lying d-band is nondegenerate; but for $\theta > 56.4°$, the doubly degenerate band lies lowest.

These observations suggest that lithium intercalation should affect the trigonal crystal-field transitions in the FTIR electronic spectrum of both $Fe_2P_2S_6$ and $Co_2P_2S_6$. However, even after 10 h of treatment at 70° with n-butyllithium, the trigonal field spectrum of $Fe_2P_2S_6$ remained unaltered. Small changes in the vibrational spectrum that have been reported previously were observed [15], but the intensity and position of the trigonal crystal-field transition remained unchanged.

The insensitivity of the FTIR electronic spectrum of $Fe_2P_2S_6$ to lithium intercalation is unexpected in view of previous experimental results indicating substantial changes in the lattice structure. For example, ^{57}Fe Mössbauer spectroscopy of $Li_xFe_2P_2S_6$ revealed the presence of two iron sites: one site essentially identical to that of the iron site in the host lattice and the other site a reduced iron with an oxidation state of zero [24]. ^{31}P NMR also demonstrates the presence of a two-phase system from the coexistence of two ^{31}P lines [25]. The result is consistent, however, with the negligible effect of lithium intercalation on the vibrational spectrum and magnetic susceptibility of $Fe_2P_2S_6$ [15]. $Li_xFe_2P_2S_6$ exhibits only a small decrease in the magnetic susceptibility upon increasing x when compared with the host lattice [3].

After treatment with n-butyllithium for less than 1 h, the FTIR electronic spectrum of $Co_2P_2S_6$ had changed dramatically. The trigonal crystal-field transition disappeared and was replaced by a strong continuous absorption edge. The tail of the absorption edge begins at about the original position of the trigonal field transition. The disappearance of the trigonal crystal-field transition and the appearance of a low-energy absorption edge in $Co_2P_2S_6$ is consistent with a transfer of electrons from the intercalated lithium to the partially occupied cobalt d-bands. The reduction of cobalt from d^7 to d^8 results in an electronic configuration isoelectronic with that of Ni^{2+} in $Ni_2P_2S_6$ that does not exhibit a trigonal field transition. Thus, the effect of lithium intercalation on the mid-IR electronic absorption spectra of $Co_2P_2S_6$ appears to support the conclusion of Whangbo *et al.* [16] that the reduction site in MPX_3 lattices during alkali–metal intercalation reactions is the low-lying partially filled $3d$-bands. However, further studies of the FTIR electronic spectrum of lithium intercalated $M_2P_2S_6$ lattices will be required before the spectroscopic effects of lithium intercalation can be interpreted with confidence.

REFERENCES

1. Klingen V. W., Ott R. and Hahn H., *Z. anorg. allg. Chem.* **396,** 271 (1973).
2. Audiere J. P., Clement R., Mathey Y. and Mazieres C., *Physica B, C,* **99,** 133 (1980).
3. Brec R., Schleich D. M., Ouvrard G., Louisy A. and Rouxel J., *Inorg. Chem.* **18,** 1814 (1979).
4. Clement R., Garnier O. and Mathey Y., *Nouv. J. Chim.* **6,** 13 (1982).
5. Covino J., Dragovich P., Lowe-Ma C. K., Kubin R. F. and Schwartz R. W., *Mater. Res. Bull.* **20,** 1099 (1985).
6. Boerio-Goates J., Lifshitz E. and Frances A. H., *Inorg. Chem.* **20,** 3019 (1981).
7. Cleary D. A., Francis A. H. and Lifshitz E., *J. Luminesc.* **35,** 163 (1986).
8. Boerio-Goates J., Lifshitz E. and Francis A. H., *Inorg. Chem.* **20,** 3019 (1981).
9. Klingen W., Eulenberger G. and Harhn H., *Z. anorg. allg. Chem.* **401,** 97 (1973).
10. Taylor B. E., Steger J. and Wold A., *J. Solid St. Chem.* **7,** 461 (1973).
11. Murphy D., DiSalvo F., Hull G. W. and Waszczak J., *Inorg. Chem.* **15,** 17 (1973).
12. Mathey Y., Clement R., Sourisseau C. and Lucazeau G., *Inorg. Chem.* **19,** 2773 (1980).
13. Sourisseau C., Forgerit J. P. and Mathey Y., *J. Phys. Chem. Solids* **4,** 119 (1983).
14. Ouvrard G., Brec R. and Rouxel J., *Mater. Res. Bull.* **20,** 1181 (1985).
15. Barj M., Sourisseau C., Ouvrard G. and Brec R., *Solid St. Ionics* **11,** 179 (1983).
16. Whangbo M.-H., Brec R. and Rouxel J., *Inorg. Chem.* **24,** 2459 (1985).
17. Mercier H., Mathey Y. and Canadell E., *Inorg. Chem.* **26,** 963 (1987).
18. Gerloch M., Lewis J., Phillips G. G. and Quested P. N., *J. chem. Soc.* **A,** 1941 (1970).
19. Gerloch M. and Quested P. M., *J. chem. Soc.* **(A),** 3729 (1971).

20. Gerloch M. and Slade R. C., *Ligand-Field Parameters*. Cambridge University Press, London (1973).
21. Jernberg P., Bjarman S. and Wappling R., *J. Magn. Magn. Mater.* **46,** 178 (1984).
22. Molinie P., Trichet L., Rouxel J., Berthier C., Charbre Y. and Segransan P., *J. Phys. Chem. Solids* **45,** 105 (1984).
23. Whangbo M.-H., Rouxel J. H. and Trichet L., *Inorg. Chem.* **24,** 1824 (1985).
24. Fatseas G. A., Evain M., Ouvrard G., Brec R. and Whangbo M. H., *Phys. Rev.* **B35,** 3082 (1987).
25. Berthier C., Chabre Y. and Minier M., *Solid St. Commun.* **28,** 327 (1978).